# RECENT RESULTS FROM PETRA ON JET FORMATION

W. BRAUNSCHWEIG

I. PHYSIKALISCHES INSTITUT

RWTH AACHEN

FR GERMANY

## I. Introduction

In this talk I will review data on the formation of hadronic jets obtained in $e^+e^-$ collisions at the PETRA storage ring. The five large detectors CELLO, JADE, MARK J, PLUTO and TASSO have contributed to this subject.

In the first part I will concentrate on the evidence on QCD coming from the analyses of the $e^+e^-$ annihilation into three (or more) hadronic jets. The combined results on energy flow, momentum flow, parton thrust, angular distributions as well as a comparison with other jet production models show that indeed the QCD model is at present the only one which gives a satisfactory description of all available data.

In the second part I will discuss the present status of the determination of the strong coupling constant $\alpha_s$. The problem here arises from the inclusion of the next to leading order corrections, $O(\alpha_s^2)$, to the one-gluon bremsstrahlung cross sections: there are two different approaches leading to different values of $\alpha_s$.

Finally I will present some results concerning the behaviour of quark and gluon jets; there are indications that quarks and gluons fragment differently: hadrons from a gluon-jet seem to have a larger mean transverse momentum (at a given jet energy) than the hadrons from a quark jet.

## II. Evidence on QCD

The hadronic final states in high energy $e^+e^-$ annihilation show predominantly a two-jet behaviour which, in the quark parton model, is explained as the process of quark pair production followed by the fragmentation (with limited transverse momentum) of these quarks into hadrons. At the highest presently available c.m. energies, $\sqrt{s} \geq 30$ GeV, a fraction of the hadronic events shows a clear three-jet-structure, which by now is well established by all five groups working at the PETRA storage ring: CELLO, JADE, MARK J, PLUTO, TASSO [1]. The occurence and the properties of these three-jet events can be well explained in the (first order) QCD model, in which the outgoing quark q (or antiquark $\bar{q}$ )radiates a hard gluon g.

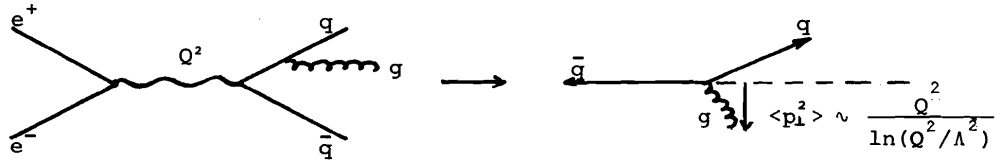

This leads to three primary partons fragmenting into hadrons. For a sufficiently large angle between the gluon and the radiating quark the hadrons appear in three well separated jets. The number of three-jet events is proportional to the running coupling constant of QCD, $\alpha_s$, and the mean transverse momentum squared of the gluon, $\langle p_t^2 \rangle_g$ is proportional to $Q^2/\ln(Q^2/\Lambda^2)$ where $Q^2$ is the momentum of the virtual photon squared, i.e. $Q^2$ equals the c.m. energy squared. Therefore, the three-jet structure becomes most distinct at the highest c.m. energies.
Of course, the underlying two- or three-jet structure has to be reconstructed from the measured hadrons. The following list contains some of the event shape measures, reconstruction methods, jet variables which have been invented for the multi-jet studies in $e^+e^-$ annihilation; only the definitions are given, the details can be found in the references (p,E are hadron momenta and hadron energies; the direction of the energy flow vector $E_i$ is given by the position of the detector element i).

1) Thrust[2] $T = \max \Sigma |p_{\parallel}| / \Sigma |p|$,
gives the value of T and the T-axis

2) Sphericity[2] $S = \min 3/2 \; \Sigma p_{\perp}^2 / \Sigma p^2$
gives the value of S and the S-axis

3) Triplicity[2] $T_3 = \max \{ |\vec{p}(C1) + \vec{p}(C2) + \vec{p}(C3)| \; / \Sigma |\vec{p}| \}$
gives the value of $T_3$ and 3-jet-axes

4) Generalized thrust[3], $F_{MA} = F_{MAJOR}$, $F_{MI} = F_{MINOR}$
Oblateness $O = F_{MA} - F_{MI}$

$$T = \max \Sigma \vec{E} \vec{e}_i / \Sigma E_i ,$$

$$F_{MA} = \max \Sigma \vec{E}_i \vec{e}_2 / \Sigma E_i$$

$$F_{MI} = \Sigma \vec{E}_i \vec{e}_3 / \Sigma E_i$$

gives values of $T, O, F_{MA}, F_{MI}$ and 3-jet-axes

5) Momentum tensor diagonalization[4]

$$M_{\alpha\beta} = p_{i\alpha} \, p_{i\beta}, \quad \alpha,\beta = x,y,z$$

with normalized eigenvalues: $Q_i$:

flatness $Q_1 = \Sigma p_1^2 / \Sigma p^2 = \langle p_{\perp}^2 \rangle_{OUT} / \langle p^2 \rangle = 2/3 \cdot A$ (A=Aplanarity)

width $Q_2 = \Sigma p_2^2 / \Sigma p^2 = \langle p_{\perp}^2 \rangle_{IN} / \langle p^2 \rangle$

length $Q_3 = \Sigma p_3^2 / \Sigma p^2 = 1 - \frac{2}{3} S$ (S = Sphericity)

where $\langle p_{\perp}^2 \rangle_{IN}$, $\langle p_{\perp}^2 \rangle_{OUT}$ are the mean transverse momenta in and out of the event plane. The method gives the values of $Q_i$.

6) Cluster algorithms [5,6]
They look for a given number of jets (clusters), e.g. for three jets:

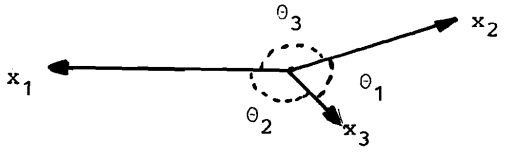

For massless partons one can calculate the fractional parton energies

$$x_i = 2E_i/\sqrt{s} = E_i/E_{beam} = 2\sin\theta_i/\Sigma\sin\theta_i$$

from the angles $\theta_i$

ordering: $\theta_1 < \theta_2 < \theta_3$ leads to

$x_1 > x_2 > x_3$

$x_1$ is identical to thrust T

The method leads to 3-jet-axes.

7) Generalized sphericity[7], which gives 3-jet-axes and the angles $\theta_1$, $\theta_2$, $\theta_3$ and correspondingly $x_1$, $x_2$, $x_3$ (s. ref. 6). The method looks for 3-jets and minimizes the sum of the three individual sphericities.

The following table gives the kind of input data, the variables and jet measures and the reconstruction methods which are used by the different groups for their jet analyses.

Table 1: Jet analyses

| Group | Input data | Variables Jet measures | Reconstruction methods |
|---|---|---|---|
| CELLO | p of charged tracks and neutral energy | $Q_1$ $Q_2$ $Q_3$<br>$x_1$<br>Oblateness | Moment.tens.diagon.<br>Cluster algorithm<br>Generalized thrust |
| JADE | p of charged tracks and neutral energy | $Q_1$ $Q_2$ $Q_3$<br>Momentum-flow<br>(p - Flow) | Moment.tens.diagon.<br>Cluster algorithm |
| MARK J | Charged and neutral energy | Major/Minor<br>Thrust<br>Energy-Flow<br>(E - Flow) | Generalized Thrust |
| PLUTO | p of charged tracks and neutral energy | Thrust<br>heavy jet mass<br>energy correl. | Thrust<br>Cluster algorithm |
| TASSO | p of charged tracks and neutral energy | $Q_1$ $Q_2$ $Q_3$<br>Thrust T<br>$x_1$ $x_2$ $x_3$ | Moment.tens.diagon.<br>Thrust<br>Generalized sphericity |

The data are compared to the predictions of QCD by using Monte Carlo event generators. Those of Hoyer et.al.[8], Ali et.al.[9] and the so called Lund model[10] are the most widely used generators. Besides the QCD matrix elements they simulate the fragmentation of the quarks and gluons into hadrons; in the first two generators the fragmentation is treated according to Feynman and Field[11], whereas the Lund generator uses a different model with the fragmentation along color strings. A detailed discussion of the generators can be found in the talk by G. Fournier at this conference[12]. The (few) parameters of these fragmentation models have been

fitted to the annihilation data (see, e.g.ref.13),especially $\sigma_q$, tne r.m.s. transverse momentum of the quark-antiquark pairs in the quark and gluon fragmentation. The first four figures display, as examples, the excellent agreement of the QCD model with the various data. Fig.1 to fig.3 have been published already;

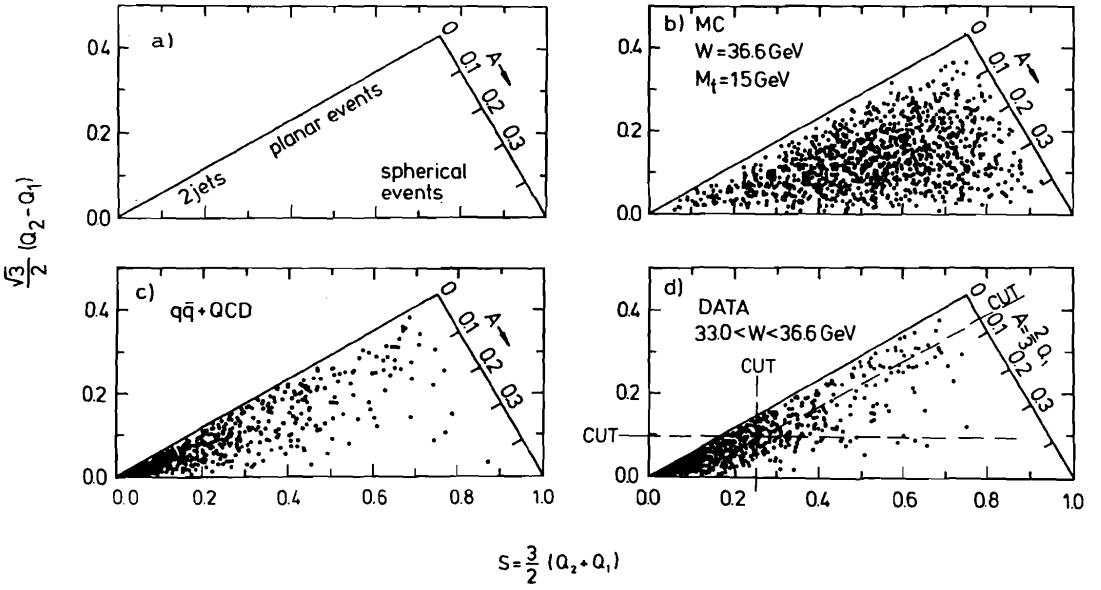


Fig.1:The event distribution in sphericity and aplanarity obtained by the TASSO group. (a) shows the regions where one expects collinear 2-jet-, coplanar 3-jet- and spherical events; (b) shows the expectation for a hypothetical top-quark with a mass $M_t$=15 GeV, and (c), (d) show the QCD expectation and the data, respectively. (d) shows cuts which are usually applied to select planar (3 jet) events.

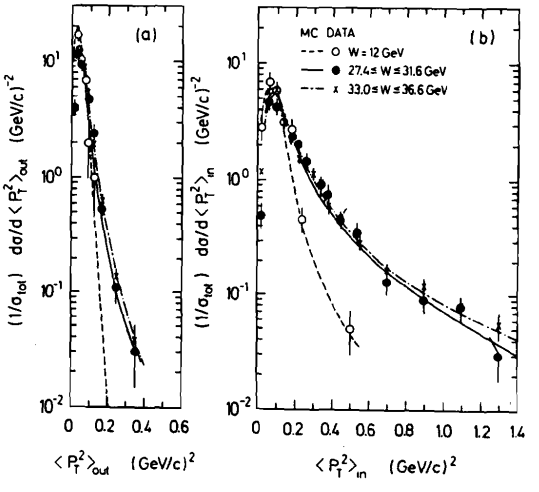


Fig.2:Distributions of mean transverse momentum squared per event for charged particles, normal to ($\langle p_\perp^2\rangle_{OUT}$) and in ($\langle p_\perp^2\rangle_{IN}$) the event plane, measured by the TASSO group at low and high energies. The curves are the predictions with $\alpha_s$=0.17 and $\sigma_q$=320 MeV/c.

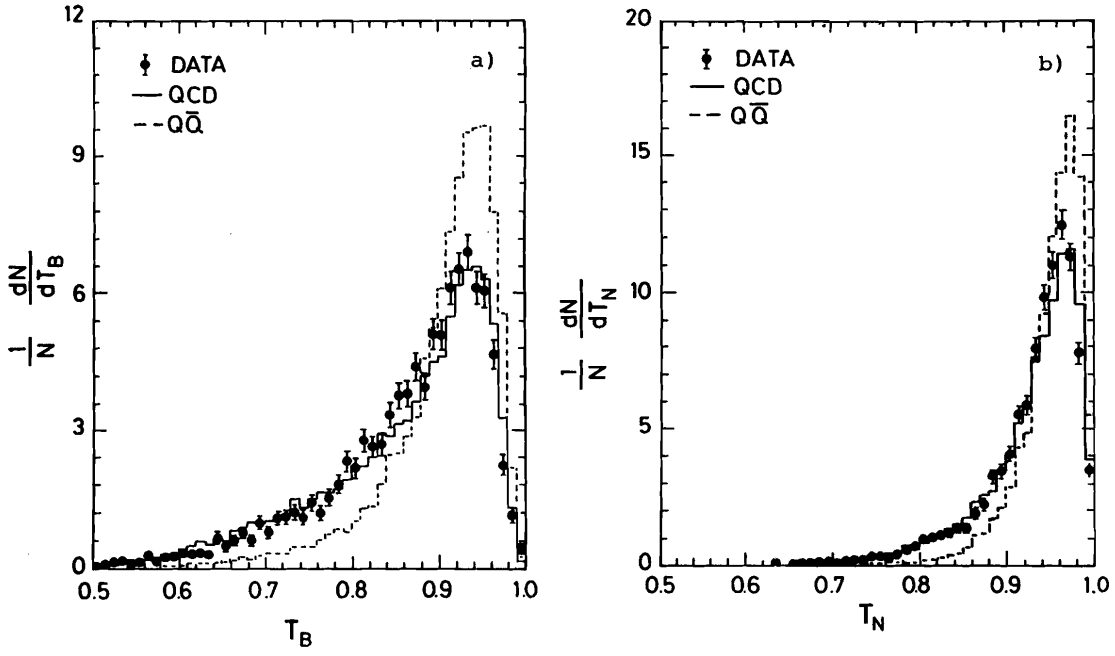


Fig.3:The distribution in broad jet thrust, $T_B$, and narrow jet thrust, $T_N$ for hadron events with $\sqrt{s} \geq 32$ GeV, compared with the predictions from the $q\bar{q}$ model and QCD; obtained by the MARK J group.

Fig.4 is a contribution from CELLO to this conference. It shows the number of jets per event obtained from a cluster analysis.

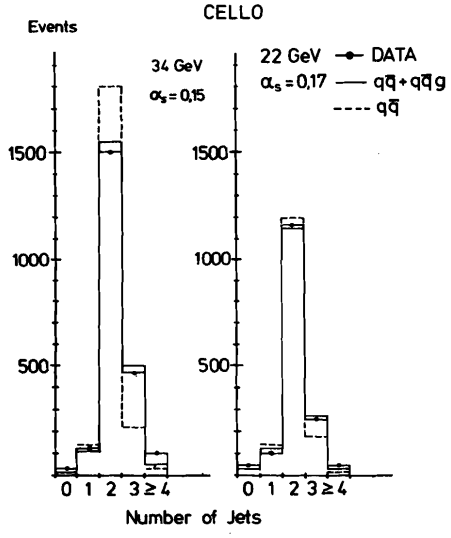


Fig.4:The distribution of the number of jets per hadronic event at two c.m. energies, compared with the predictions from a $q\bar{q}$ model and QCD, obtained by the CELLO group.

Especially at 34 GeV the expected numbers from the QCD-($q\bar{q}$ + $q\bar{q}g$) model are in good agreement with the data. The predicted numbers in the $q\bar{q}$ model, where 3-jet and 4-jet events are due to the reconstruction algorithm and fluctuations in the fragmentation, are far too low.

Special studies on selected 3-jet events have been done in order to look for alternatives to QCD. Fig. 5 shows the MARK J result, for events with broad jet oblateness[14] $O_B > 0.3$, on the energy flow $1/E\ dE/d\phi$, compared with various models. Only the QCD model is able to describe the whole distribution correctly. A modified $q\bar{q}$ model with an additional exponential tail exp $(-q_\perp/650$ MeV) in the fragmentation function does not reproduce the 3-peak structure. On the other hand, the distribution of the broad jet oblateness $O_B$ alone (fig.6) is well reproduced by the modified model. This clearly demonstrates that one has to compare the detailed features of the data with the models, and not only one single distribution.

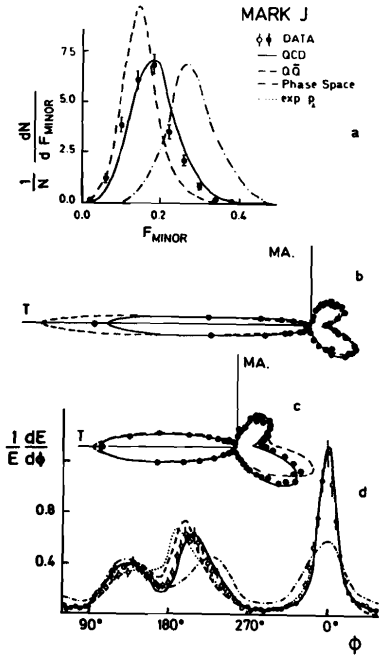


Fig.5: (a) The distribution $1/N\ dN/dF_{MINOR}$, perpendicular to the event plane for 3-jet events, i.e. Oblateness $O_B > 0.3$.
(b), (c) energy flow diagrams for 3-jet events and (d) unfolded energy flow diagram of fig.5b , obtained by the MARK J group. The data are compared with the models of QCD, a $q\bar{q}$ model with an exponential tail in the transverse momentum fragmentation function, the normal $q\bar{q}$ model and phase space.

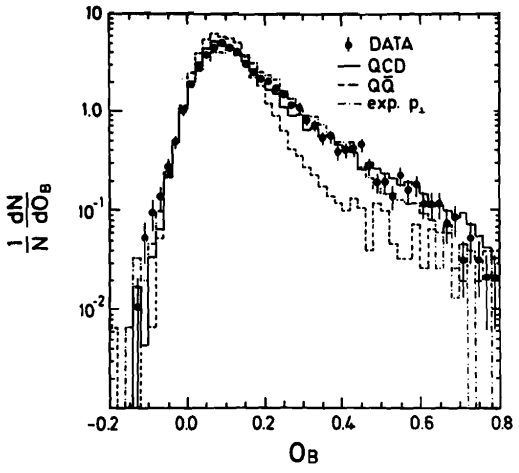


Fig.6:The broad jet oblateness distribution $1/N\ dN/dO_B$, obtained by MARK J. The data are compared with the models of QCD, $q\bar{q}$ and the modified $q\bar{q}$ model (see fig.5)

The JADE group has presented data on the momentum flow. The analysis was performed in the following steps:

- 3-jet-cluster analysis on selected 3-jet events (cut $Q_2-Q_1>.07$, see fig.1d)
- calculation of hardest jet #1 from angles between the jets
- event plane defined by jet #2 and jet #3
- 0°-direction defined by projection of jet #1 on to event plane
- projection of each track, charged or neutral, on to event plane
- track angle $\Theta$ defined with respect to jet 1.

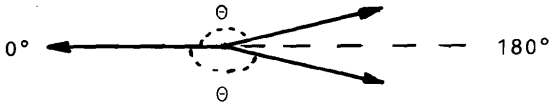


The resulting momentum flow distribution $1/\Sigma p\ dp/d\Theta$ is symmetric around $\Theta = 180°$. Fig.7 shows the distribution together with the QCD prediction, which perfectly describes the two-peak structure around 180°, i.e. the dip at 180°. The $q\bar{q}$ model fails drastically: it gives too few 3-jet events and - for the cut $Q_2-Q_1>0.07$-it does not reproduce the dip at 180°.However,as fig.8 shows, with a tighter cut on $Q_2-Q_1$, i.e. selecting events which are more planar and which have larger sphericities (see fig.1d) the $q\bar{q}$ model also starts to reproduce the two peak structure around 180°.

The TASSO group has presented special studies on 3 jet events. They reconstruct the 3 jets by applying the generalized sphericity method, leading to the directions of the 3 jet axes in a plane. From the ordered angles $\Theta_1<\Theta_2<\Theta_3$ between the axes the fractional energies $x_i = 2\ E_i/\sqrt{s} = 2 \sin\Theta_i/\Sigma \sin\Theta_i$ are calculated, leading to $x_1>x_2>x_3$; fig. 9 shows a Dalitz plot of the TASSO data. A cut on the parton thrust $x_1<0.9$ selects then events with 3 well separated jets: the lowest energetic jet has

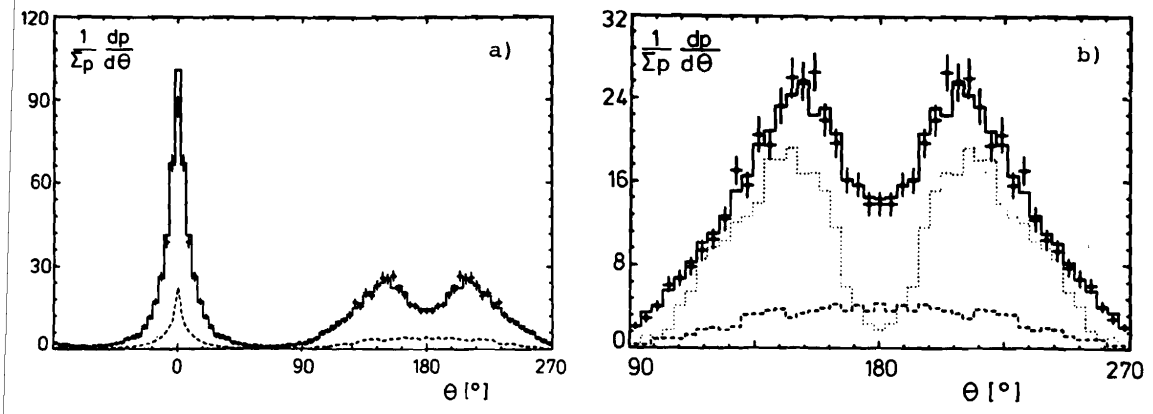


Fig.7: (a) The unfolded momentum flow distribution $1/\Sigma_p \cdot dp/d\theta$, obtained by the JADE group. The data are compared with the models of QCD (solid curve) and $q\bar{q}$ (dashed curve).
(b) same as (a), but on an extended scale; the dotted curve shows the parton distribution, i.e. the momentum flow before fragmentation of the quarks and gluons.

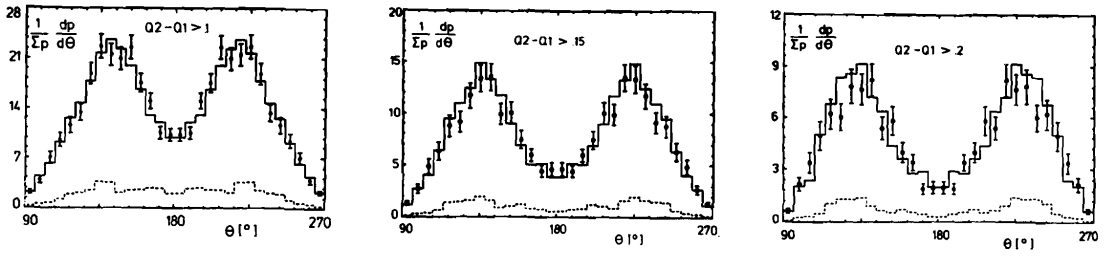


Fig.8: The unfolded momentum flow distribution in three different regions of the sphericity-aplanarity plot, selected by a cut on $Q_2-Q_1$ (see fig.1). Obtained by the JADE group; curves as in fig.7.

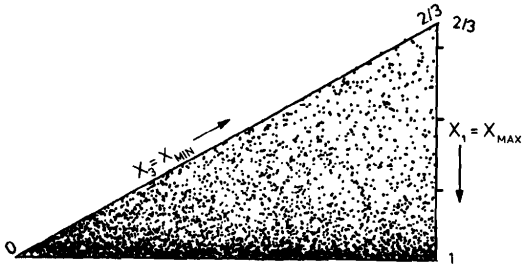


Fig.9: Distribution of all TASSO data above 25 GeV in the Dalitz plot of the fractional parton energies $x_i = 2E_i/\sqrt{s}$, calculated from the angles $\theta_i$ between the jet axes. The condition $\theta_1<\theta_2<\theta_3$ and consequently $x_1>x_2>x_3$ restricts the Dalitz plot to the triangular region shown in the figure.

always $x_3 > 0.2$ (typically $x_3 = 0.4$) corresponding to $E_3 > 3$ GeV (typically $E_3 = 6$ GeV); the jet opening angle is $2\delta_3 < 50°$, whereas the minimum angle between any two jets is $\Theta_1 \geq 70°$. The following table shows the results of Monte Carlo studies, made by the TASSO group, on the precision with which the 3 jet axes are reconstructed:

Table 2: Precision of reconstruction

| | r.m.s. difference (per event) | | | systematic bias (all events-average) | | |
|---|---|---|---|---|---|---|
| | $\Theta_1$ | $\Theta_3$ | $x_1$ | $\Theta_1$ | $\Theta_3$ | $x_1$ |
| Hadronization radiative corrections detector acceptance | 18° | 12° | 0.07 | -2° | -1° | -0.012 |
| charged + neutrals versus charged alone | 7° | 8° | 0.04 | +1° | 0° | -0.002 |
| reconstructed jet axes versus $\sum_{Jet} \vec{p}_{Hadron}$ | 6° | 4° | 0.02 | -3° | 0° | +0.008 |

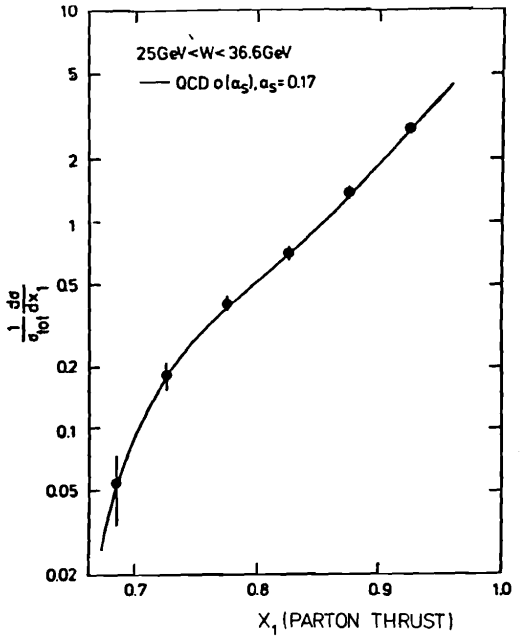


Fig.10: The parton thrust distribution obtained by the TASSO group. The solid curve represents the QCD calculation to leading order in $\alpha_s$ with $\alpha_s = 0.17$.

Fig.10 shows the parton thrust ($x_1$) distribution, obtained by the TASSO group. The QCD prediction ($O(\alpha_s)$ with $\alpha_s = 0.17$) agrees exceedingly well with the data. Fig.11, fig.12, fig.13 and the following table summarize the TASSO results on the comparison of their data with various 2-jet models.

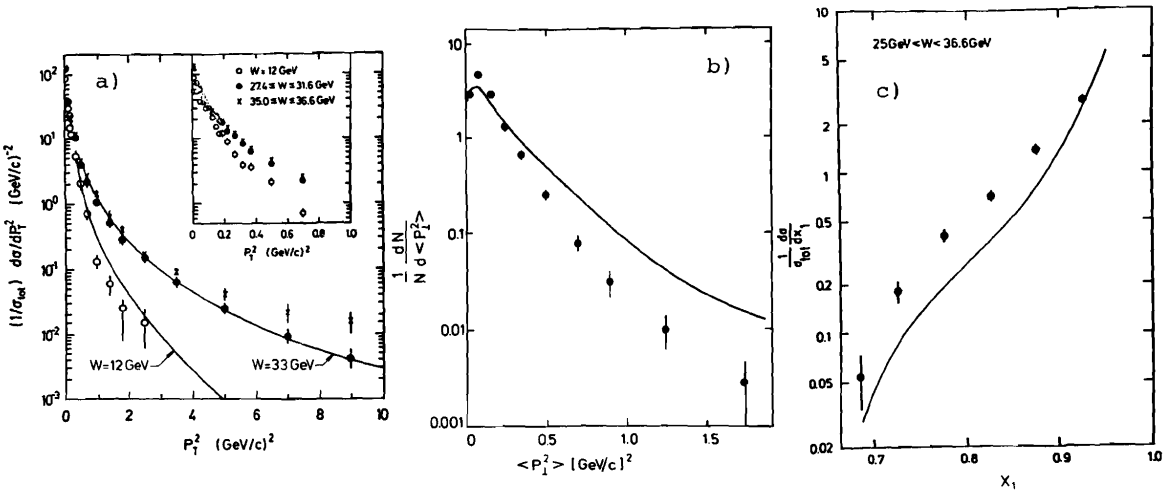


Fig.11: (a) The distribution of the transverse hadron momenta squared w.r.t. the sphericity axis of the whole events at low and high energies. The curves represent a fit to the distribution with a modified $q\bar{q}$-model with $\sigma_q$=320 MeV/c for the light quarks u,d,s and $\sigma_Q$=800 MeV/c for the heavy quarks c,b.
(b) The distribution of the mean transverse momentum squared in each of the 3 jets of the events w.r.t. the corresponding jet axes. The curve is the prediction of the same model as in fig.11a.
(c) The parton thrust distribution. The curve is the prediction of the same model as in fig.11a. Fig.11 was presented by the TASSO group.

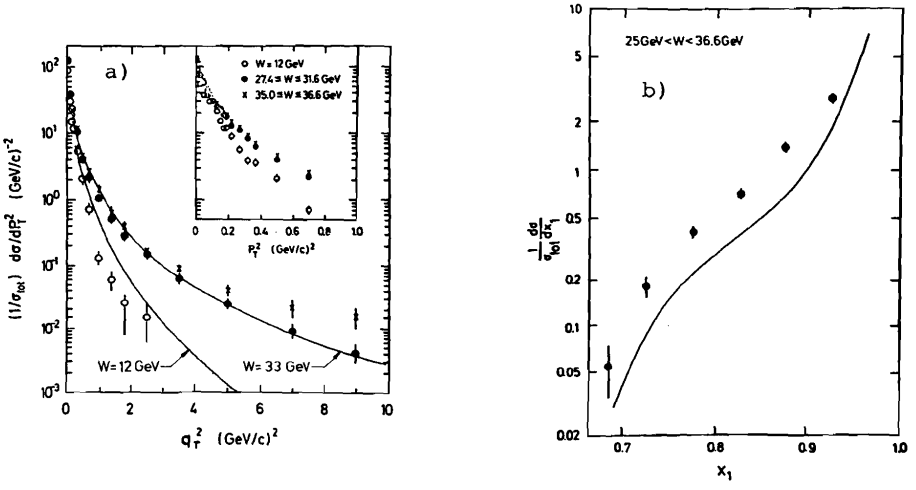


Fig.12: (a) The same distribution as in fig.11a. The curves represent a fit to the distribution with a modified $q\bar{q}$-model with a $q_T^{-4}$-power tail in addition to the gaussian distribution for the $q_T$-quark and gluon fragmentation functions
(b) The parton thrust distribution. The curve is the prediction of the same model as in fig.12a. Fig.12 was presented by the TASSO group.

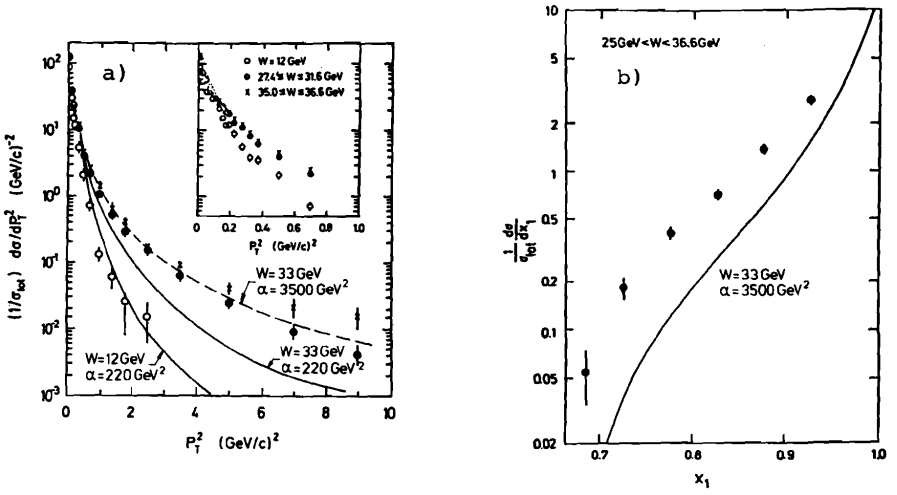


Fig.13: (a) The same distribution as in fig.11a. The curves represent calculations of a CIM-model with the indicated values for the $q\bar{q}$-meson coupling constant $\alpha$
(b) The parton thrust distribution. The curve is the prediction of the same model (as in fig.13a with the indicated value for the coupling constant $\alpha$
Fig.13 was presented by the TASSO group.

Table 3: Comparison with 2 jet models

| Model | Result | |
|---|---|---|
| $d\sigma/dq_\perp^2 \sim \exp(-q_\perp^2/2\sigma_q^2)$<br>$\sigma_q$ = 320 MeV/c for u,d,s<br>$\sigma_q$ = 800 MeV/c for c,b | $p_\perp^2$, $\langle p_\perp^2\rangle_{IN}$, $\langle p_\perp^2\rangle_{OUT}$ good<br>$x_1$ too low<br>$p_\perp^2$ w.r.t. 3 axes too broad | fig.11 |
| $d\sigma/dq_\perp^2 \sim \exp(-q_\perp/a)$ | $p_\perp^2$, $\langle p_\perp^2\rangle_{IN}$, $\langle p_\perp^2\rangle_{OUT}$ good<br>$x_1$ too low | |
| $d\sigma/dq_\perp^2 \sim \exp(-q_\perp^2/2\sigma_q^2)$<br>+ a $q_\perp^{-4}$ | $p_\perp^2$, $\langle p_\perp^2\rangle_{IN}$, $\langle p_\perp^2\rangle_{OUT}$ good<br>$x_1$ too low | fig.12 |
| CIM, Higher twist [23] | $p_\perp^2$ wrong energy dependence<br>$x_1$ too low | fig.13<br>fig.15 |

$q_\perp$ is the transverse momentum of the quarks in the fragmentation cascade.

To conclude: All models which have been considered so far in order to replace QCD have failed to reproduce all features of the data. Of course, there might be small additional contributions from other processes (higher twist) and/or slight modifications of the fragmentation functions. The TASSO group estimates the higher twist contributions to be less than 10%, which is in agreement with an earlier estimate of PLUTO [15].

New information has been presented on the question of the gluon spin. Fig.14 shows the parton thrust distribution obtained by the CELLO group. From the comparison with the vector and scalar gluon hypothesis it clearly follows that the data strongly favour the gluon spin to be one. The same conclusion can be drawn from the parton thrust ($x_1$) and transverse parton thrust ($x_\perp$) distributions obtained by the PLUTO group (fig.15).

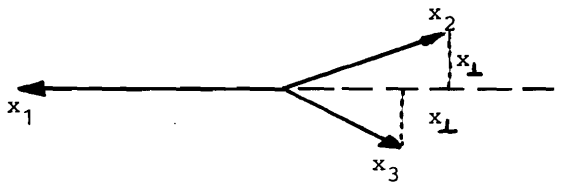


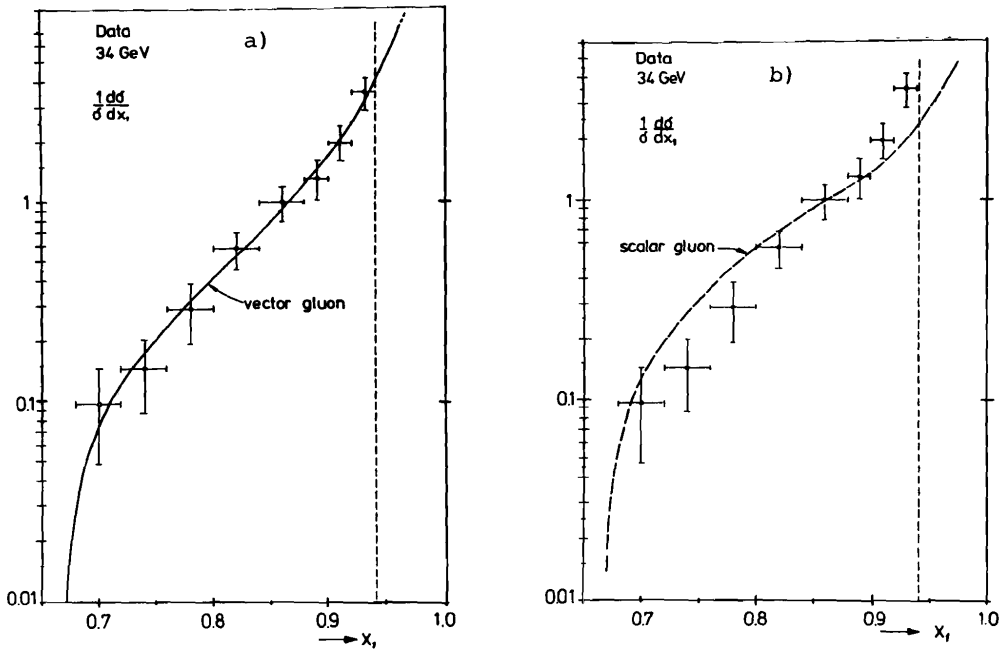


Fig.14: The distribution of the parton thrust $x_1$ at a mean c.m. energy of $\sqrt{s}$=34 GeV, obtained by the CELLO group. The curve is the leading order QCD prediction for vector gluons (a) and a prediction for a scalar gluon model (b).

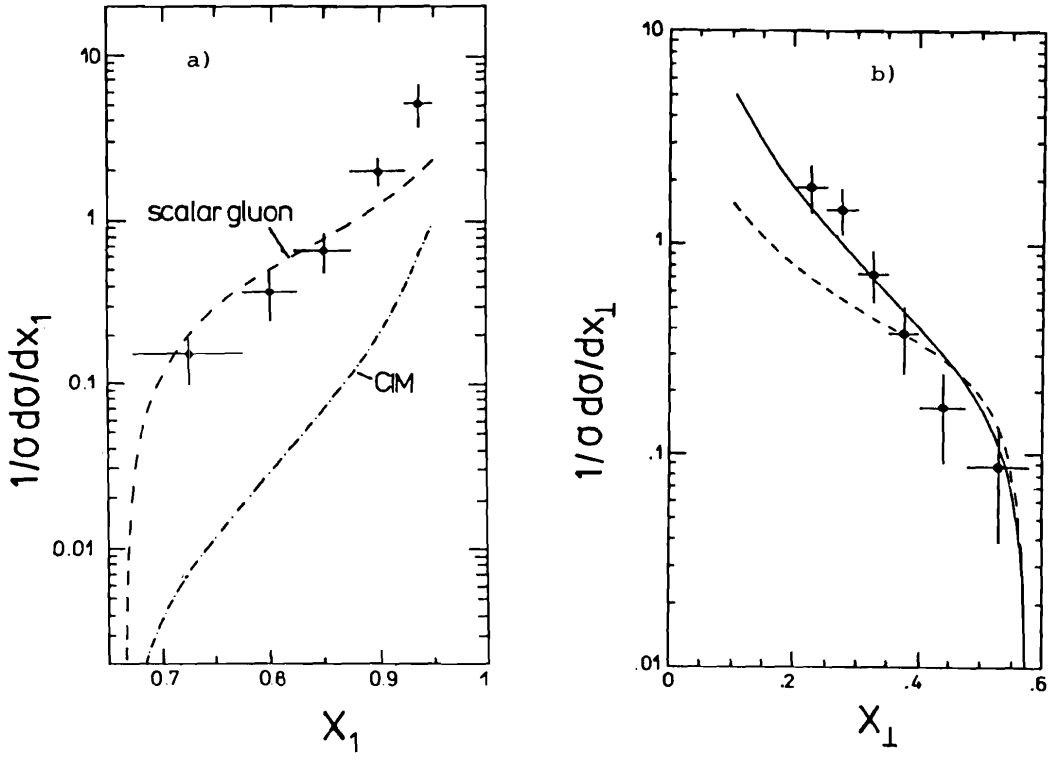


Fig.15: (a) The distribution of the parton thrust $x_1$ at $\sqrt{s}$ = 30 GeV, obtained by the PLUTO group. The curves show predictions of the CIM model and a scalar gluom model. (b) The distribution of the fractional transverse energy $x_\perp$ of the low and medium energetic partons w.r.t. the most energetic parton direction. The solid curve is the QCD prediction, the dashed curve is the prediction of a model with scalar gluons.

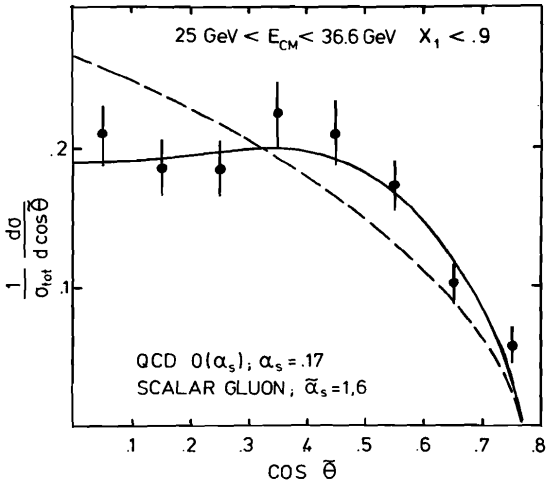


Fig.16: The distribution of the Ellis-Karliner angle $\tilde{\Theta}$ for the 3-jet events ($x_1 < 0.9$), obtained by the TASSO group. The full curve represents the leading order QCD prediction with $\alpha_s = 0.17$. The dashed curve is the prediction of a scalar gluon model with $\tilde{\alpha}_s = 1.6$.

The TASSO group presented the distribution of the Ellis-Karliner[16] angle $\cos\tilde{\Theta}$ with improved statistics (fig.16).

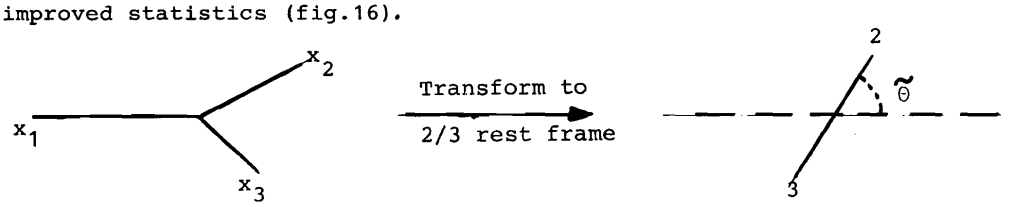


The comparison of the experimental mean value

$$\langle\cos\tilde{\Theta}\rangle_{EXP} = 0.3391 \pm 0.0079$$

with the QCD expectation

$$\langle\cos\tilde{\Theta}\rangle_{EXP} - \langle\cos\tilde{\Theta}\rangle_{QCD} = 0.0019 \pm 0.0084$$

and the expectation from a scalar gluon model

$$\langle\cos\tilde{\Theta}\rangle_{EXP} - \langle\cos\tilde{\Theta}\rangle_{\text{scalar gluon}} = 0.0411 \pm 0.0084$$

rules out the scalar gluon hypothesis (confidence level $1 \cdot 10^{-6}$).
The QCD model predicts for the distribution of the angle $\Theta_T$ of the overall thrust axis a form proportional to $1 + \alpha(T)\cdot\cos^2\Theta_T$, where $\alpha(T)$ decreases with decreasing thrust T.

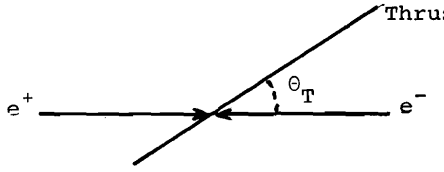


An indication of this effect has been seen by the TASSO group. Fig.17 shows the angular distribution in two different thrust regions together with parametrizations proportional to $1 + \alpha(T)\cos^2\Theta T$, where $\alpha(T)$ has been fitted. The results are $\alpha(0.9 \leq T \leq 1.0) = 1.00 \pm 0.11$ (QCD expectation 0.97) and $\alpha(T \leq 0.9) = 0.75 \pm 0.18$ (QCD expectation 0.77). The agreement is good, but one clearly needs more statistics in order to get the detailed behaviour of $\alpha(T)$.

III. Status of the determination of $\alpha_s$.

Table 4 displays the results on $\alpha_s$ of all five PETRA detectors. These results are valid to first order, i.e. the Monte Carlo generators which have been used to obtain them, contain QCD matrix elements to order $O(\alpha_s)$. The first errors are statistical, the second errors (if quoted) are systematic. The results are not completely independent of the fragmentation; the main correlation exists between $\alpha_s$ and $\sigma_q$. The uncertainty due to this correlation is contained in the errors.

Table 4: First order results on $\alpha_s$

| Group | $\alpha_s$ | $\sqrt{s}$ |
|---|---|---|
| JADE | $0.18 \pm 0.03 \pm 0.03$ | |
| MARK J | $0.17 \pm 0.02$ | at ~ 30 GeV |
| PLUTO | $0.16 \pm 0.02$ | |
| TASSO[22] | $0.19 \pm 0.01 \pm 0.03$ | |
| CELLO | $0.15 \pm 0.015 \pm 0.025$ | at 34 GeV |

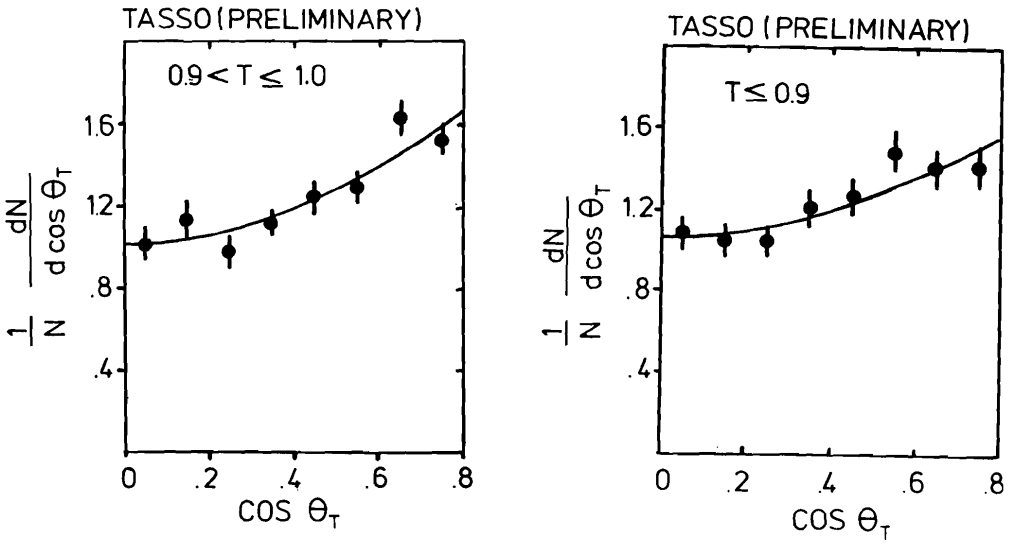


Fig.17: The distribution of the polar angle of the thrust axis, $\cos\Theta_T$ in the $e^+e^-$ c.m. system, for $T \leq 0.9$ and $0.9 < T < 1.0$. The curves are fits to the data of the form $1+\alpha_T(T)\cos^2\Theta_T$. Fig.17 was presented by the TASSO group.

At present the second order QCD effects cannot be included uniquely, because there exist two models (model I[17] and model II[18]) which do not give the same results. The models are not rigorously comparable, because they calculate different quantities. (The main problem lies in the separation of 3- and 4-jet events: model I uses a Sterman Weinberg-type separation, whereas model II uses a bare thrust variable). However, in order to get an indication of the size of the second order effects, fig.18 displays the overall thrust distribution to $O(\alpha_s)$ as well as the distributions including the $O(\alpha_s^2)$ for both models ($\alpha_s = 0.157$).
Using the model I the TASSO group has performed a complete analysis including $O(\alpha_s^2)$ (i.e. changing the Monte Carlo generator as well as the reconstruction algorithm) for the $x_{max}$ (=max $x_1, x_2, x_3$) distribution, which is shown in fig.19. Taking the $\overline{MS}$ renormalization scheme, the fitted value is $\alpha_s = 0.17$.
The authors of model I[17] have performed a similar analysis on the PLUTO data: fig.20 shows their result on the 3-jet-cross section, versus $x_{max}$. Taking again the $\overline{MS}$ scheme, the fitted value is $\alpha_s = 0.17$.
On the other hand, analyzing the TASSO data using model II, Ali [19] gets a value $\alpha_s = 0.128$.

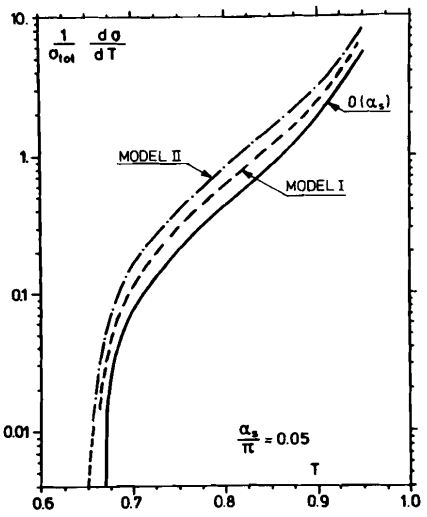


Fig.18: The QCD prediction for the reconstructed thrust T to leading order (full curve, indication $O(\alpha_s)$). Also shown are the QCD predictions of the two models which include the second order $O(\alpha_s^2)$ effects.

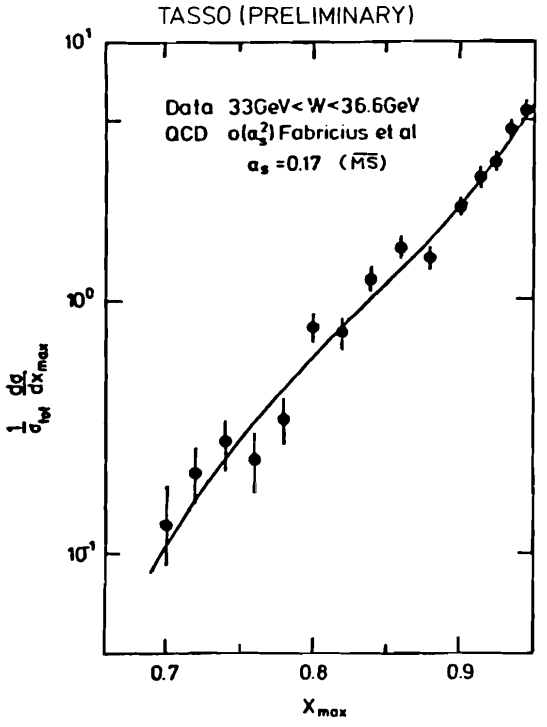


Fig.19: The cross section as a function of the $x_{max}=\max(x_1,x_2,x_3)$, obtained by the TASSO group. The curve is the QCD prediction for $\alpha_s=0.17$ including the second order effects on the $\overline{MS}$ renormalization scheme according to the model of Fabricius et al. (ref. (17)).

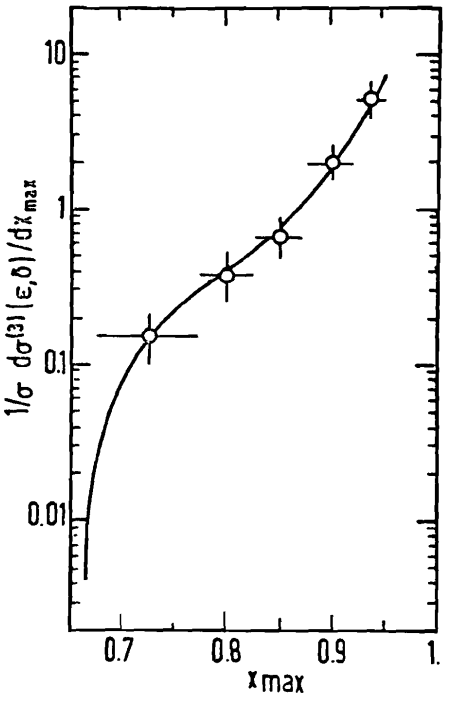


Fig.20: The 3 jet cross section as a function of $x_{max}=\max(x_1,x_2,x_3)$ obtained by the PLUTO group. The curve is the QCD prediction for $\alpha_s = 0.17$ including the second order effects. Same model as in fig.19.

The PLUTO group has taken a different approach by studying the energy dependence of various jet measures:

- mean thrust <T> or 1- <T>
- energy weighted jet broadness [20] $\langle \sin^2\eta \rangle$

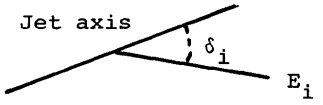


$$\sin^2 \eta_i = E_i \sin^2\delta_i/\sqrt{s}$$

- heavy jet mass [21] $\langle M_H^2/s \rangle$
- energy-energy-correlations [20] in the central region: $\int_{60°}^{120°} f(\Theta)d\Theta$

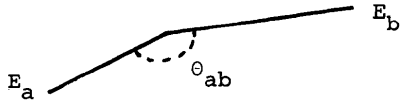


$$f(\Theta) = \sum_a \sum_b E_a E_b/s \cdot \Theta(\Theta_{ab}-\Theta)$$

The idea is that each of these observables takes the form

$$\langle Obs \rangle = A \cdot \alpha_s/\pi + B/\sqrt{s}$$

where the first term is due to QCD and A is calculable (at least to $O(\alpha_s)$), and the

second term is due to the fragmentation and B can be expressed in terms of the mean charged multiplicity $\langle n_{CH} \rangle$, the mean $\langle p_\perp \rangle$ etc.
Fig.21 shows the PLUTO data together with the fits according to the above formula, leading to $\alpha_s$ values between 0.16 und 0.20, in agreement with the PLUTO value $\alpha_s = 0.18$ at $\sqrt{s} = 30$ GeV, as obtained from the 3 jet studies.

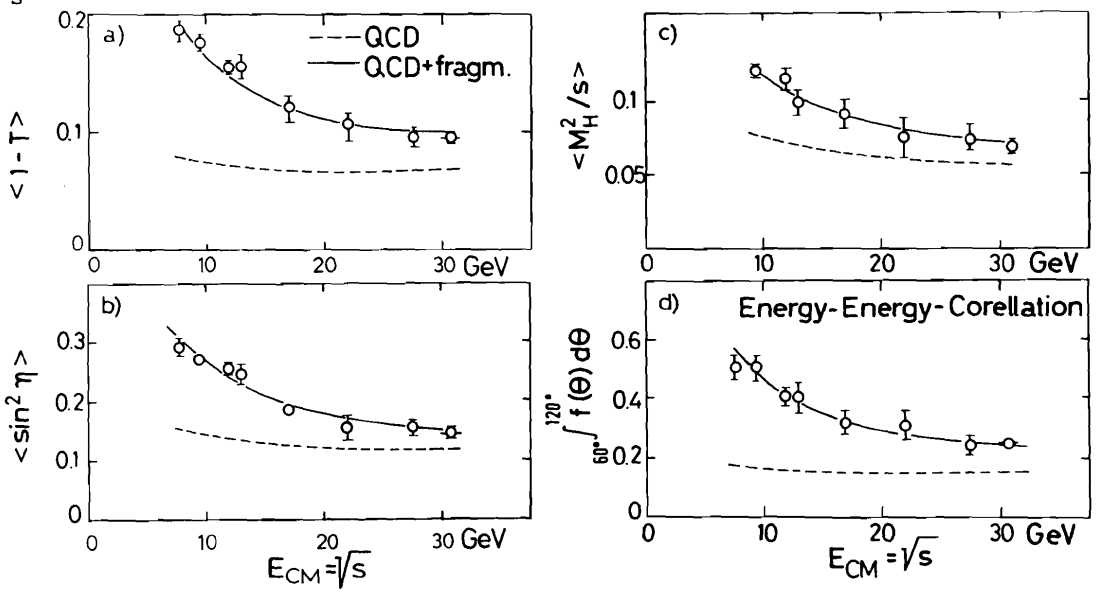


Fig. 21: Energy dependence of various jet measures, obtained by the PLUTO group; (a) 1-Thrust T; (b) jet opening angle η; (c) normalized heavy jet mass $M_H^2/s$; (d) energy-energy correlations. The curves are described in the text.

To conclude this section: the situation with respect to the second order QCD contributions to the 3-jet cross sections is unsatisfactory and needs clarification from theory. The uncertainty of $\alpha_s$ due to the second order contributions amounts to $\sim$ 0.05. Therefore at present it seems impossible to calculate a reliable value for the QCD cut off parameter $\Lambda$ by using $\alpha_s$.

IV. Are quark and gluon jets different?

Due to the possibility of the three gluon coupling one expects that the opening angle of a gluon jet is broader than that of a quark jet:

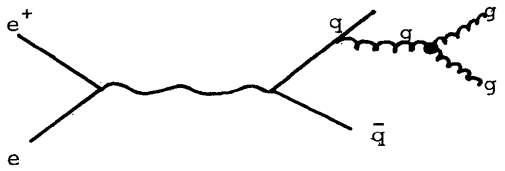


As a consequence, the mean transverse momentum of the hadrons originating from a gluon should be larger (in, $\langle p_\perp \rangle_{IN}$ as well as out, $\langle p_\perp \rangle_{OUT}$, of the event plane) than the corresponding quantities of a quark jet.
In their 3-jet-sample the JADE group has seen indications for this effect: At a given visible jet energy, the values $\langle p_\perp \rangle$, as well as $\langle p_\perp \rangle_{OUT}$, of the lowest energy jet are significantly larger than the corresponding values for the other two

jets. According to Monte Carlo studies, the lowest energy jet is preferentially (50%) the gluon jet.
The effect does not seem to be due to reconstruction algorithms: In a simulation using the Hoyer et.al. Monte Carlo generator, which does not contain second order terms, the effect is not reproduced (see the curves in fig.22). On the other hand, a simulation using the Lund-Monte-Carlo-generator in which gluon and quark fragmentation are treated differently shows at least part of the effect (curves in fig.23, the data are the same as in fig.22).

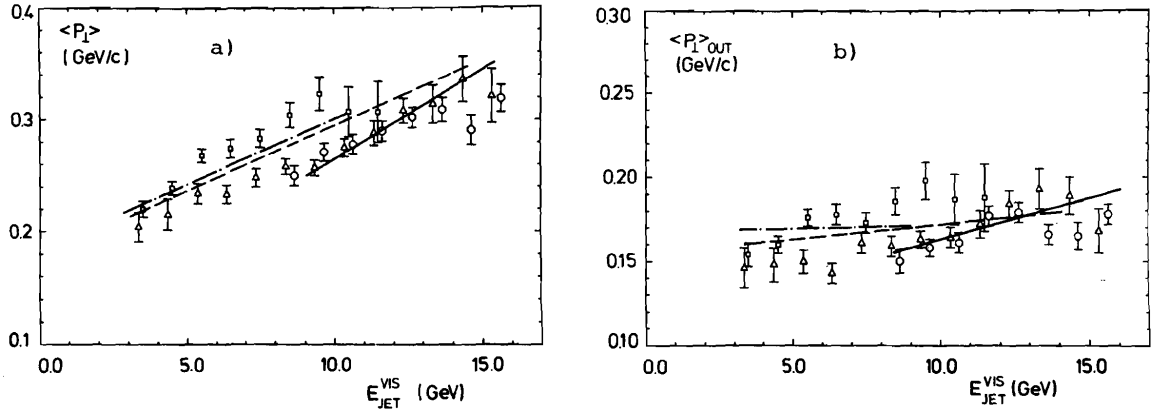


Fig.22: (a) The mean transverse momentum of the hadrons in the highest energy jet (● and full curve) the next to highest energy jet (◐ and dashed curve) and the lowest energy jet (○ and dashed-dotted curve) versus the visible energy in that jet, as obtained by the JADE group for the selected three jet events. The curves represent predictions of the event generator of Hoyer et.al. (b) Same as fig.22a, but for the mean transverse momentum out of the event plane.

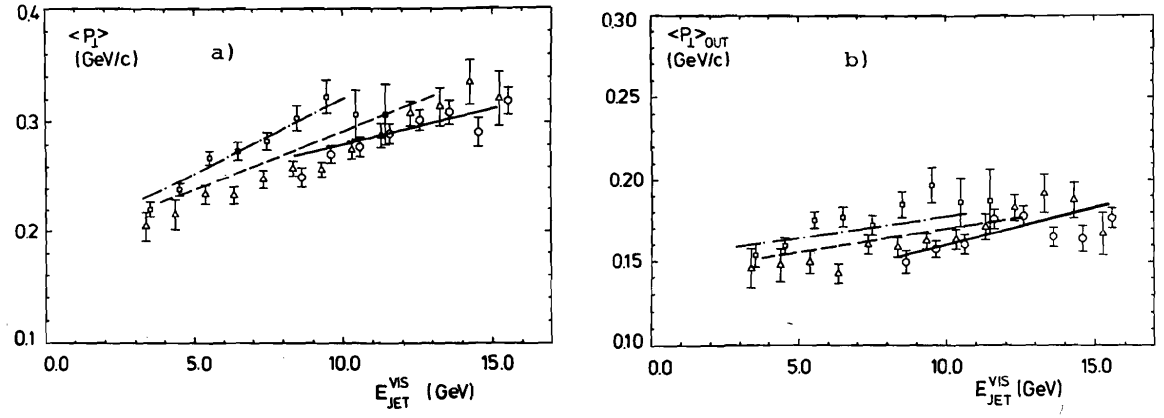


Fig. 23 (a), (b): The same data as in figs. 22a, 22b. The curves represent the predictions of the event generator of the LUND group.

The $< p_\perp >$ behaviour of the highest energetic and medium energetic jet corresponds to that of quark jets. This is shown in fig.24, (the data are again the same as in fig.22) where the full line represents a fit to the $< p_\perp >$ distribution of selected 2-jet-events, i.e. of quark jets.

However, the effect is not confirmed by the MARK J group: Fig.25 shows the angular distribution of the energy flow for jet #1 and jet #3. The distribution is not much different for jet #3 at 35 GeV (preferentially the gluon jet) and jet #1 at 14 GeV (quark jet).

To conclude this section: the effect seen by the JADE group needs further study; especially the effect of second order contributions (i.c. 4 jet events) needs an investigation.

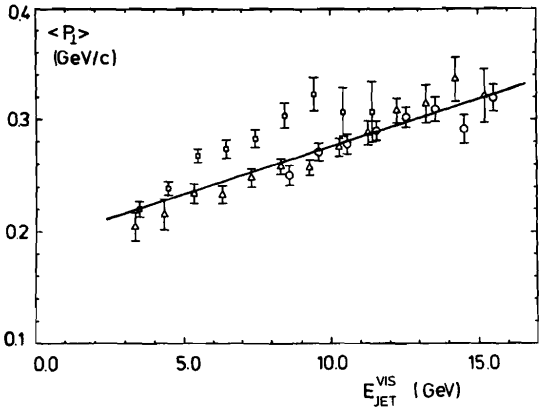


Fig.24: The same data as in fig.22a, 23a. The curve shows a fit to the $< p_\perp >$ of the selected 2-jet events.

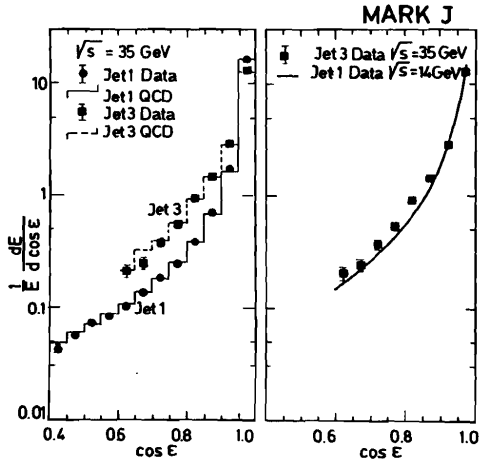


Fig.25: The angular distribution of the energy flow with respect to each of the three jet axes, as obtained by the MARK J group. The curves are QCD predictions (left figure). In the right figure the behaviour of the most energetic jet at low c.m. energies is compared to that of the lowest energetic jet at high c.m. energies.

## V. Conclusion

- QCD, including fragmentation, describes all observed properties of the hadronic final states in high energy $e^+e^-$ annihilation very well.
- QCD is necessary,
  $q\bar{q}$-models with modified fragmentation fail to reprocedure all observed features of the data.
- $O(\alpha_s^2)$ contributions to 3 jet cross sections are not settled satisfactory.
  model I : $\alpha_s \sim 0.17$
  model II: $\alpha_s \sim 0.12$.
- Scalar gluons are ruled out (Confidence level $1 \cdot 10^{-6}$).
- Different behaviour of gluon- and quark jet needs confirmation.

I would like to thank my scientific secretaries H. G. Sander and L. Köpke.
I am grateful to J. Bürger, D. Fournier, M. Goddard, K. Lübelsmeyer, A. Petersen, P. Söding, G. Wolf for very useful discussions and for support.

## References

1. I refer to the excellent review article "Experimental Evidence on QCD" by P. Söding and G. Wolf:
   DESY report 81/013 and to be published in "Annual Review of Nuclear Science".
   The article contains the most recent and complete list of references.
2. Brandt, S., Dahmen, H.D.:
   Z. Physik C1 (1979), 61
3. Mark J Collaboration, Barber, D.P. et.al.:
   Physics Reports 63 No.7 (1980), 337
4. A detailed description can be found in ref. 1
5. Daum, H.J., Meyer, H., Bürger, J.:
   DESY report 80/101 and Z. Physik C8 (1981), 167
6. Dorfan, J.:
   SLAC-PUB-2623 and Z. Physik C7 (1981), 349
7. Wu, S.L., Zobernig, G.:
   Z. Physik C2 (1979), 107
8. Hoyer, P. et.al.:
   Nucl. Phys. B161 (1979), 349
9. Ali, A. et. al.:
   Z. Physik C2 (1979), 33; Phys.Lett. 83B (1979), 375; Phys.Lett. 93B (1980),155; Nucl.Phys. B168 (1980), 409

10.Andersson, B., Gustafson, G., Sjöstrand, T. :
Phys. Lett. 94B (1980), 211 and references quoted therein
11.Field, R.D., Feynman, R.P. :
Nucl.Phys. B138 (1978), 1
12.Fournier, D.:
"Recent results from PETRA on production of neutral particles",
proceedings of this conference, P.
13.Tasso Collaboration, Brandelik, R. et.al. :
Phys. Lett. 94B (1980), 437
14.Mark J Collaboration, Barber,P. et.al. :
M.I.T. - L.N.S. report No. 115 (1981)
15.Daum, H.J. :
Ph.D.thesis (1981), Gesamthochschule Wuppertal (unpublished)
16.Ellis,J., Karliner, I. :
Nucl.Phys. B148 (1979), 141
17.a)Fabricius, K. et.al. :
Phys. Lett. 97B (1980), 431
b)Fabricius, K. et.al. :
preprint DESY 81/035 (1981)
18.a)Ellis, R.K., Ross, D.A., Terrano, A.E. :
Phys. Rev. Lett. 45(1980), 1226; CAL-Tech. Rep. 68-785 (1980);
Nucl. Phys. B178 (1981), 421; Phys. Lett. 106B (1981),88
b)Vermaseren, J.A.M., Gaemers, K.J.F., Oldham, S.J. :
CERN Rep. TH 3002 (1980); Nucl. Phys. 187 (1981), 301
c)Kunszt, Z.:
Phys. Lett. 99B (1981), 429
19.Ali, A. private communication
20.Basham, C.L. et.al.:
Phys. Rev. Lett. 41 (1978), 1585; Phys. Rev. D17 (1979), 2298;
Phys. Rev. D19 (1979), 2018
21.a)Clavelli, A. Wyler,D.:
Phys. Lett. 103B (1981), 383
b)Chandramehan, T., Clavelli, L.:
Nucl. Phys. B184 (1981), 365
22.The TASSO value which is given in table 4 was obtained with first order terms.
For the published TASSO value $\alpha_s = 0.17 \pm 0.02 \pm 0.03$ (ref.13) second order terms
were included (see also ref.1)
23.De Grand, T.A.; Ng. Y.J.; Tye, S.H.H.:
Phys. Rev. D16 (1977), 3251

Discussion

G. Karl, Guelph Univ.: You gave the confidence level of a fit for scalar gluons as $10^{-6}$. What is the confidence level of the fit with vector gluons?

P. Söding, DESY: The agreement of the Ellis-Karliner angular distribution measured by TASSO, with QCD is perfect: the $\chi^2$ is 6 at 7 degrees of freedom.

K. Kleinknecht, Univ. of Dortmund: You showed the result of two different theoretical calculations on the thrust distribution. Model I gives $\alpha_s = 0.17$, and the second order contribution is small. For model II the second order contribution is very large (30%-50%). As long as it is not clear which of these is correct, is it legitimate to extract $\alpha_s$ at all? If the second order contribution is large indeed, the third order could be even larger.

W. Braunschweig: As I said, the problem of the second order contributions needs clarification from theory. The extraction of $\alpha_s$ is useful because it allows the comparison of different data and of various methods by which QCD is tested. Concerning the last part of your question: to my knowledge nobody has tried yet to calculate the third order.

G. Barbiellini, CERN: In the $p_\perp$-analysis for 3-jet events from JADE: How is the visible jet energy defined?

W. Braunschweig: It is the sum of the neutral and charged energy.